Received 30 January 2019; revised 22 April 2019; accepted 23 August 2019. Date of publication 27 August 2019; date of current version 30 September 2019.
The review of this article was arranged by Editor M. Mouis.

Digital Object Identifier 10.1109/JEDS.2019.2937916

UTBB-Based Single Transistor Image Sensor of Submicron Pixel Using Back Gate Modulation

LIQIAO LIU, XIAOYAN LIU (Member, IEEE), AND GANG DU (Member, IEEE)

Key Laboratory of Microelectronic Devices and Circuits, Institute of Microelectronics, Peking University, Beijing 100871, China

CORRESPONDING AUTHOR: G. DU (e-mail: gangdu@pku.edu.cn)

This work was supported in part by the National Key Research and Development Plan under Grant 2016YFA0202101, and in part by the National Natural Science Foundation of China under Project 61674008.

ABSTRACT Image sensor has developed for decades. Now, submicron photo sensor device with high performance is required. In this work, a UTBB (ultra-thin body and box) based single transistor image sensor has been investigated. The light collection and signal readout are accomplished by a single transistor, so the pixel of the UTBB image sensor can shrink down to the submicron. The main parameters impacting the performance of the UTBB image sensor such as back voltage, the thickness of the BOX, well doping concentration and well depth are investigated. Besides, the UTBB image sensor can achieve multi-resolution to adapt to different requirements. The performance of the UTBB image sensor is evaluated by TCAD simulations.

INDEX TERMS UTBB image sensor, submicron pixel size, back gate modulation.

I. INTRODUCTION

Image sensors have been widely used in various areas [1]. Image sensors have undergone pixel size reduction, performance improvement and structural optimization for decades [2], [3]. With the development of process technology, image sensors have been scaling down to meet the increasingly demanding requirements. In some advanced applications such as bioimaging, super-resolution microscopy is required [4]. Recently, an 8K imaging system was applied to endoscopic surgery [5]. In order to obtain high resolution, the pixel size of the image sensor is continuously scaling down [6]. In the traditional CMOS image sensor (CIS), for the purpose of better noise performance, the pixel is composed of a photodiode, reset transistor, driver of the source-follower and addressing transistor [7], [8]. However, the fill factor of the conventional 3-T (three transistors) CMOS image sensors is inferior. Some works have been done to improve the fill factor. For example, in CMOS image sensor implemented with three dimensional (3D) integration technology, most of the data processing circuit and the pixel array is fabricated in different layers, and the signals can be transferred between the layers through the interconnection. Thus the fill factor of the pixel can almost reach 100% [9]. However, there are some potential limitations to 3D integration technology, such as the heating effect within the stack and the complexity of design and process [10]. Another way to improve the fill factor is developing 1-T (one transistor) image sensor. Image sensors without charge transfer have been studied extensively and various new structures where the photo-generated charge signal can be magnified and read directly, have been proposed [11]–[13].

UTBB device has developed for better gate-control ability and reduced leakage current [14]. The back gate modulation can be used to adjust threshold voltage (Vth) [15], [16], which can be applied to image sensing. By integrating UTBB and photodiode, some researchers proposed a new image sensor which achieves light collection and signals magnifying within one transistor [17]. The photodiode below the BOX is used to collect optical signal and the photo-generated carriers create a light-induced V_T shift in both NFET & PFET transistors by means of capacitive coupling. Such 1-T image sensor can realize both higher fill factor and better scalability.

In this work, we propose and demonstrate a 1-T UTBB image sensor, which converts light signal to electric signal using back bias induced threshold voltage modulation. Upon illumination, the photo-generated charges will be stored

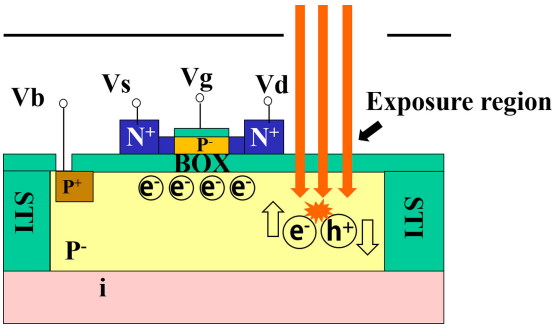

FIGURE 1. The schematic of the 1-T UTBB image sensor structure.

under the BOX, changing the threshold voltage and ON-state drain current of the MOSFET. When the pixel is selected, the gate voltage is applied and the drain current of the pixel is read out. Thus the light intensity is evaluated. Back voltage is applied to reset the UTBB for the next round of light detection. As a result, our UTBB sensor achieves light collection, signal magnifying and read out in a single MOSFET, allowing the pixel to scale to hundreds of nanometers.

TCAD tool Sentaurus [18] is used to investigate the performance of our UTBB image sensor. The drift-diffusion model, Philips unified mobility model, high field saturation models and Shockley–Read–Hall (SRH) generation recombination model are used for electrical simulation. Raytracing method is adopted for optical simulation.

The rest of the paper is organized as follows: In Section II, the device structure and operation principle are introduced. In Section III, the simulated electrical characteristics of the UTBB image sensor are presented. Finally, conclusions are given in Section IV.

II. DEVICE STRUCTURE AND MECHANISM

The pixel cell structure of the UTBB image sensor is shown in Fig. 1. A p-well is formed in the undoped silicon substrate and an n-channel UTBB transistor is placed above the well. For the sake of better light absorption, the incident light can only pass through the exposure region to avoid light absorption in the transistor. After penetrating the BOX, photons are absorbed by the p-well under the exposure region and converted into photo-generated carriers. Around the pixel, SiO2 shallow trench isolation (STI) surrounding the p-well is used to suppress crosstalk between pixels. The main structure parameters are shown in Table 1.

The UTBB image sensor has four main operation stages: initialization, exposure, readout and reset. Table 2 shows the bias conditions under different operation stages. Before each detection cycle, the image sensor should be reset to clear the carriers generated in the previous cycle. After reset, the image sensor is initialized and all terminals are biased to 0V. During exposure, Vd is set to 0.8V and Vb to -0.8V, i.e., Vdb $= +1.6$V. An electric field is set up inside the p-well, where the absorbed photons are converted into photo-generated carriers. The photo-generated electrons move towards the BOX under the electric field. Note that the

TABLE 1. Structure parameters of the UTBB image sensor.

Parameter(Unit)	Value
Channel length (nm)	30
Silicon thickness (nm)	6
EOT (nm)	1
BOX thickness (nm)	10
Well depth (nm)	500
Exposure region width (nm)	200
Channel doping (cm^{-3})	$5x10^{16}$
Drain & source doping (cm^{-3})	$1x10^{20}$
Well doping (cm^{-3})	$5x10^{16}$

TABLE 2. Bias conditions in different operation stages.

	Initial	Exposure	Readout	Reset
V_g (V)	0	0	0.8	0
V_d (V)	0	0.8	0.8	0
V_s (V)	0	0	0	0
V_b (V)	0	-0.8	-0.8	0 or 1.6

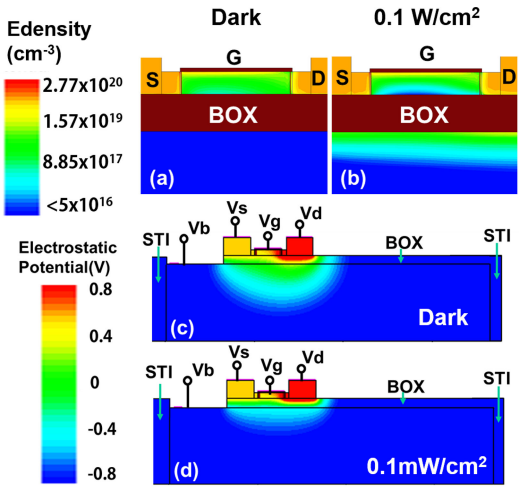

FIGURE 2. (a) (b) The electron density distribution of the UTBB image sensor under dark and illuminated condition. (c) (d) The electrostatic potential distribution of the UTBB image sensor under dark and illuminated condition.

electrostatic potential under the BOX becomes more negative due to the carriers' accumulation. Fig. 2 (a) (b) shows the electron density distribution of the UTBB image sensor under dark and illumination condition respectively. Fig. 2 (c) (d) illustrates changes in potential distribution caused by carriers' accumulation. To better describe the change of potential under BOX, we define Vif as the electrostatic potential of the interface between BOX and p-well right below the middle of the channel. Under dark condition, Vif is 0.21V whereas under the light intensity of 100μW/cm^2, Vif drops to -0.46V.

The change of the electrostatic potential under BOX works as back gate modulation and increases the threshold voltage

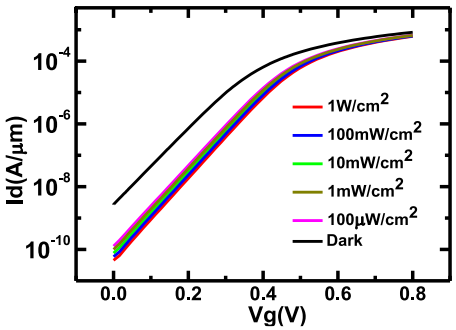

FIGURE 3. Transfer characteristics of the UTBB image sensor under dark and different light condition.

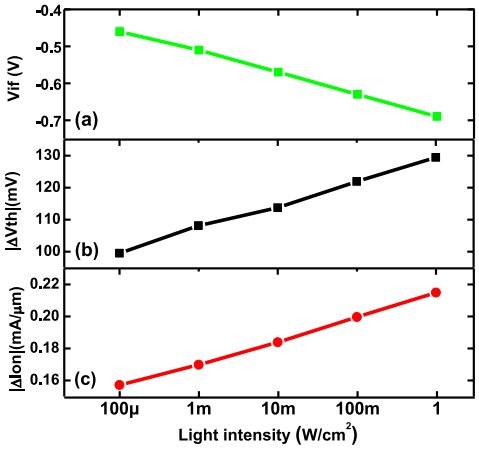

FIGURE 4. Relationship between light intensity and Vif, |ΔVth| and |ΔIon|.

of the MOSFET above. In the readout stage, when the gate voltage is applied, due to the shift of threshold voltage, the ON-state current of the transistor would decrease after illumination. After readout, the device is reset again for the next cycle of detection. Intuitively, Vb is set to 1.6V with Vd = 0V to reverse Vdb in the exposure and readout stage. However, the device can also be reset when Vdb is 0V, which will be explained in Section III in detail.

The transfer characteristics of the UTBB image sensor under dark and different illuminated conditions (550nm; varying light intensity) are plotted in Fig. 3. The threshold voltage of the NMOS increases after illumination. As the light intensity increases, the threshold voltage increases continuously. Fig. 4 shows the relationship between light intensity and Vif, |ΔVth| and |ΔIon|. Vth is extracted at a constant |Id| = 10^{-8}A/μm. As the light intensity increases, Vif declines continuously. Consequently, the |ΔVth| rises from 99.5mV to 129.4mV and |ΔIon| increases from 0.157mA/μm to 0.215mA/μm. Therefore, the light intensity is measured by detecting |ΔIon|.

III. RESULTS AND DISCUSSION

A. IMPACT OF THE BACK VOLTAGE ON PERFORMANCE

As explained before, the photo-generated carriers are driven by the back voltage Vb. Thus, the accumulation of the photo-generated carriers is strongly dependent on the back voltage. Vb is changed to obtain different Vdb (Vs is set to 0V and Vd is set to 0.8V to keep Vds = 0.8V). As the Vdb increases, more photo-generated electrons gather under the BOX and the shift of Vif is greater. Fig. 5 shows Vif changing during illumination with different Vdb. With Vdb = 0.8V, the shift of Vif is 0.24V, which increases to 1.34V, when Vdb = 2.4V. Fig. 6 shows the Id changes during the illumination with different Vdb. Similarly, |ΔIon| increases with higher Vdb. In other words, increasing Vdb effectively improves the sensitivity of our image sensor.

Fig. 7 shows the Vth with different Vdb under dark and light illumination. When Vdb = 0.8V, Vth is 10mV in dark and 48mV after illumination. With Vdb = 2.4V, Vth

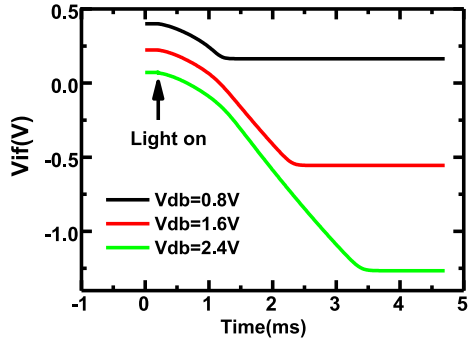

FIGURE 5. Vif changes with different Vdb. Illumination begins at time = 0.2ms. The light intensity is 10mW/cm^2 and the wavelength is 550nm.

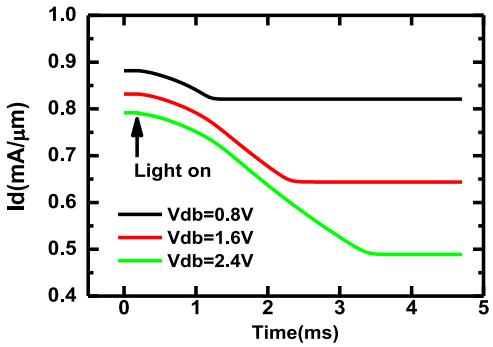

FIGURE 6. Id changes with different Vdb. Illumination begins at time = 0.2ms. The light intensity is 10mW/cm^2 and the wavelength is 550nm.

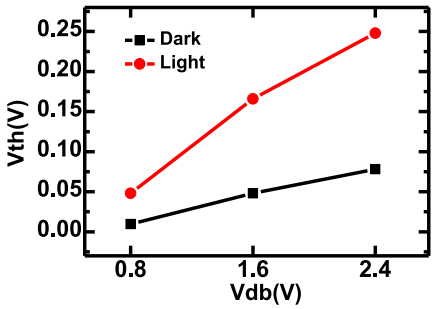

FIGURE 7. Vth changes with different Vdb under dark and illuminated condition. The light intensity is 10mW/cm^2 and the wavelength is 550nm.

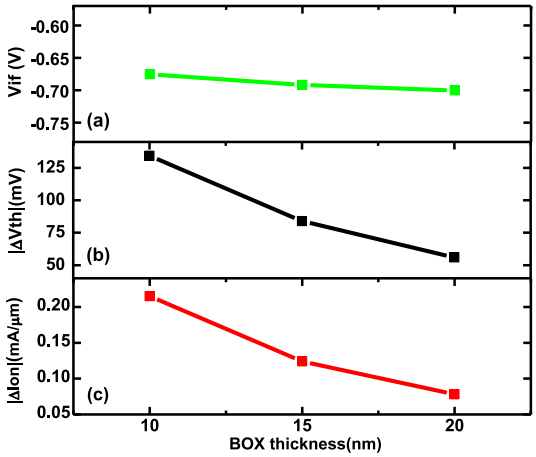

FIGURE 8. Vif, |ΔVth| and |ΔIon| after illumination with different BOX thickness. The light intensity is 1W/cm^2, and the wavelength is 550nm.

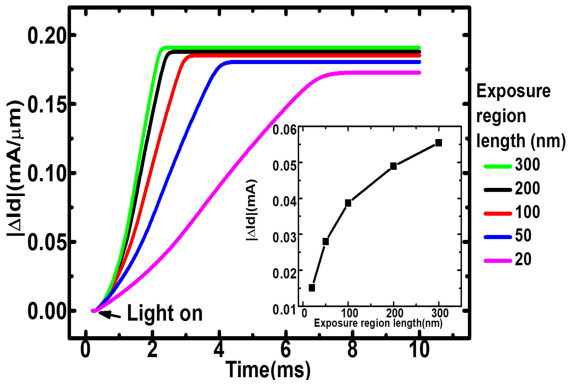

FIGURE 9. |ΔId| changes during illumination with different exposure region length. The light intensity is 10mW/cm^2 and the wavelength is 550nm.

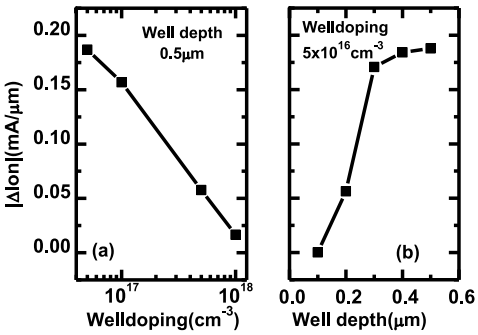

FIGURE 10. The relationship between |ΔIon| and (a) well doping concentration and (b) well depth. The light intensity is 10mW/cm^2 and the wavelength is 550nm.

increases to 78mV and 248mV in dark and after illumination respectively. The shift of Vth due to illumination is greater with larger Vdb, which also proves the improvement of sensitivity with higher Vdb.

B. IMPACT OF THE BOX THICKNESS ON PERFORMANCE

The thickness of the BOX also plays an important role in determining device performance. The back gate modulation caused by the accumulation of photo-generated carriers under the BOX is the key to the performance of our UTBB image sensor, and the BOX thickness has decisive influences on the back gate modulation. Fig. 8 shows the Vif, |ΔVth| and |ΔIon| after illumination with different BOX thickness. Despite different BOX thickness, Vif is basically the same due to the same light condition. However, the electrostatic potential under BOX can produce more back gate modulation with thinner BOX. As a result, the light sensitivity can be improved by thinner BOX, which is illustrated in Fig. 8 (b) and (c), with 20nm BOX, the |ΔVth| and |ΔIon| are 55.9mV and 0.078mA/μm after illumination. As the thickness of the BOX reduces to 10nm, |ΔVth| and |ΔIon| are improved to 134.3mV and 0.215mA/μm.

C. IMPACT OF EXPOSURE REGION ON PERFORMANCE

The length of the exposure also has an important influence on performance. Fig. 9 shows the |ΔId| changes during illumination with different exposure region length. Under the same light condition, the length of the exposure region has little impact on the Id shift. On the other hand, the response times are more sensitive to exposure region length. As exposure region length increases, the response time of Id becomes shorter. The inset shows the |ΔId| at 1ms after light on. With larger exposure region, the pixel can collect more photons in a short time, so the Id changes faster. However, larger exposure region will lead to an increase in the pixel area. Therefore, the optimized pixel size should depend on the specific application.

D. IMPACT OF WELL DOPING AND WELL DEPTH ON PERFORMANCE

The photons are mainly absorbed and converted into photon-generated carriers in the doping well under the BOX. Hence, the well doping concentration and the well depth have a great impact on the performance. Fig. 10 shows |ΔIon| dependence on well doping concentration and well depth. With high well doping concentration |ΔIon| caused by illumination is smaller. Since the photon-generated carriers are mainly collected at the depletion region of the p-well, high doping level results in smaller depletion region thereby lowering the collection efficiency. Similarly, the well depth also impacts the light sensitivity by influencing the depletion region. When well depth $< 0.3\mu$m, |ΔIon| increases rapidly with the well depth. However, when well depth $> 0.3\mu$m, |ΔIon| tends to saturate. That means that the depletion width has reached the maximum $\sim 0.3\mu$m at the given doping concentration of 5×10^{16} cm^{-3}. To sum up, the well doping concentration should be lower and well should be deep enough to get better light sensitivity.

E. PERIODIC WORKING PROCESS OF UTBB IMAGE SENSOR

Fig. 11 shows the drain current change in one detection cycle under dark and illuminated condition. During the

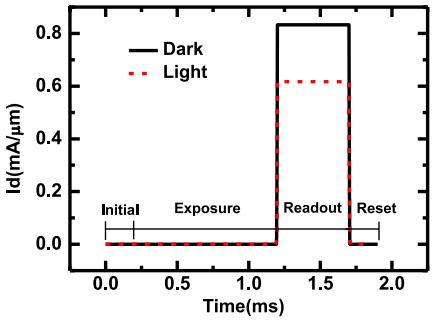

FIGURE 11. Drain current of the UTBB image sensor over a detection cycle under dark and light. The light intensity is 1 W/cm^2 and the wavelength is 550nm.

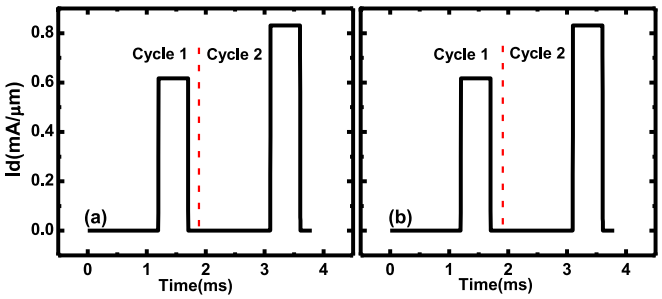

FIGURE 12. Id changes in two consecutive cycles with different reset voltage. (a) Vdb = −1.6 V in reset stage. (b) Vdb = 0 V in reset stage.

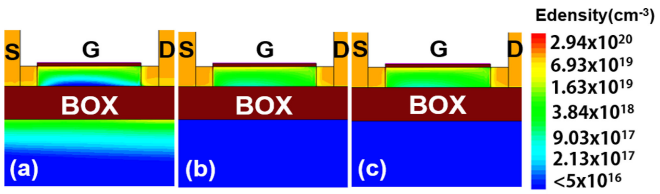

FIGURE 13. Electron density of the UTBB image sensor at different conditions. (a) Illuminated (b) Reset by Vdb = −1.6 V (c) Reset by Vdb = 0V.

readout stage, the current difference between dark and light (0.2mA/um) is sufficiently large to be distinguished by the peripheral circuit.

In order to achieve continuous operation, the reset process of the UTBB image sensor needs to be investigated. Fig. 12 compares the reset process with different Vb in reset stage. The reset voltage Vdb is −1.6V and 0V in Fig. 12 (a) and (b) respectively. The image sensor is illuminated in Cycle 1 and kept in dark in Cycle 2. The readout current in Cycle 2 is basically equal in these two cases, implying that their reset effects are basically the same. This can be explained by Fig. 13, which shows the electron density under the BOX after reset.

As shown in Fig. 13, after illumination, the high electron density can only be maintained when the Vdb is negative enough. It is found that the electrons accumulated under the BOX will be cleared no matter Vdb = −1.6V or 0V, because when Vdb = 0V or more positive, the electron density under the BOX will drop abruptly and the potential under the BOX

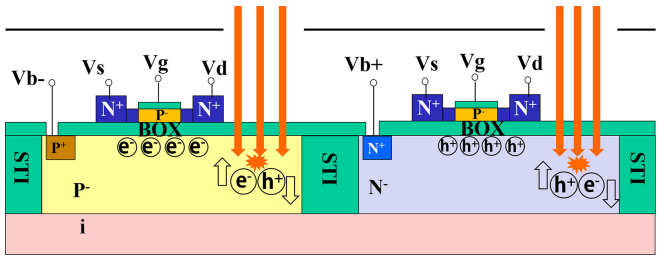

FIGURE 14. The pixel cell structure of the complementary UTBB image sensor.

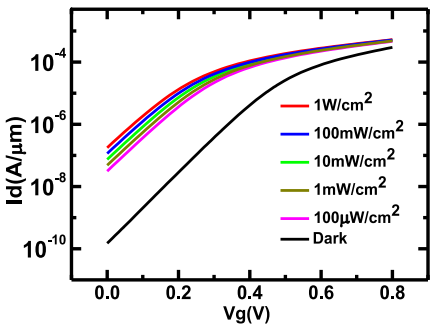

FIGURE 15. Transfer characteristics of the n-well UTBB image sensor under dark and different light condition. The wavelength is 550nm.

is reset, i.e., Vdb = 0V is enough for reset. Therefore, the detection cycle can be simplified by combining initial and reset into one stage.

F. COMPLEMENTARY UTBB IMAGE SENSOR WITH MULTI-RESOLUTION

The complementary UTBB image sensor is composed of two UTBB single transistor image sensors with different doping-type wells as shown in Fig. 14. The structure parameters and bias condition of the n-well transistor are the same as the p-well transistor, except the back voltage.

Opposite to that in p-well, the Vdb in n-well transistor is negative, which drags the photo-generated holes towards the BOX. That will raise the electrostatic potential under the BOX. Consequently, the threshold voltage of the NMOS will decrease. The transfer characteristics of the n-well UTBB image sensor under dark and different illuminated condition are plotted in Fig. 15.

In Fig. 15, the threshold voltage of the NMOS decreases after illumination. As the light intensity increases, the threshold voltage decreases continuously. The phenomenon is opposite to that of the p-well device. By detecting differential current I_{diff} between complementary UTBB image sensors, the light sensitivity can be improved. Fig. 16 shows I_{diff} in one detection cycle under dark and illuminated condition. Compared with Fig. 11, the change of differential current between dark and illuminated condition is more significant. Thus the complementary UTBB image sensor can achieve better light sensitivity by sacrificing a little resolution.

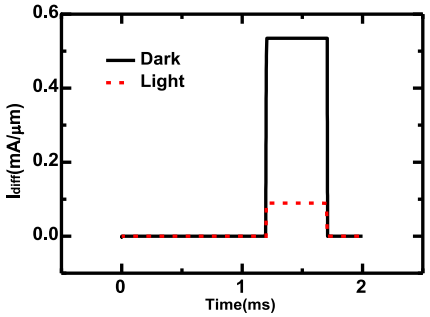

FIGURE 16. **The differential current between complementary UTBB image sensors in one detection cycle under dark and illuminated condition.**

Since the complementary UTBB image sensor can also be divided into two independent 1-T UTBB image sensors, it can work flexibly in either high-resolution mode, or high-sensitivity mode. In high-resolution mode, every single transistor UTBB image sensor works independently. In high-sensitivity mode, two complementary transistors are grouped into a larger pixel where the light sensitivity is improved by detecting differential current.

IV. CONCLUSION

In this paper, we have designed a novel UTBB image sensor which achieves submicron pixel resolution. The device is based on the back gate modulation caused by photo-generated carriers in the well. The impact of back voltage, BOX thickness, well doping concentration, well depth and exposure region length on the device performance have been studied in the simulation. The operation scheme of the device and complementary sensor capable of multi-resolution have also been proposed.

REFERENCES

[1] J. Ohta, *Smart CMOS Image Sensors and Applications*. Boca Raton, FL, USA: Taylor & Francis, 2008.

[2] E. R. Fossum and D. B. Hondongwa, "A review of the pinned photodiode for CCD and CMOS image sensors," *IEEE J. Electron Devices Soc.*, vol. 2, no. 3, pp. 33–43, May 2014.

[3] H.-S. Wong, "Technology and device scaling considerations for CMOS imagers," *IEEE Trans. Electron Devices*, vol. 43, no. 12, pp. 2131–2142, Dec. 1996.

[4] A. E. Willner *et al.*, "Optics and photonics: Key enabling technologies," *Proc. IEEE*, vol. 100, pp. 1604–1643, May 2012.

[5] K. Tanioka, "8K imaging systems and their medical applications," in *Proc. Int. Image Sensor Workshop*, 2017, pp. 348–351.

[6] J. C. Ahn *et al.*, "Advanced image sensor technology for pixel scaling down toward 1.0μm (Invited)," in *Proc. IEEE Int. Electron Devices Meeting (IEDM)*, 2008, pp. 1–4.

[7] A. J. P. Theuwissen, "CMOS image sensors: State-of-the-art," *Solid-State Electron.*, vol. 52, no. 9, pp. 1401–1406, 2008.

[8] P. Magnan, "Detection of visible photons in CCD and CMOS: A comparative view," *Nucl. Instrum. Methods Phys. Res. A Accelerators Spectrom. Detect. Assoc. Equip.*, vol. 504, nos. 1–3, pp. 199–212, 2003.

[9] R. Bonnard, F. Guellec, J. Segura, A. Dupret, and W. Uhring, "New 3D-integrated burst image sensor architectures with in-situ A/D conversion," in *Proc. IEEE Design Archit. Signal Image Process.*, 2013, pp. 215–222.

[10] D. Zhang and J.-Q. Lu, "3D integration technologies: An overview," in *Materials for Advanced Packaging*. Cham, Switzerland: Springer Int., 2017.

[11] X.-Y. Liu *et al.*, "A novel single-transistor APS and its comparison with 3T CMOS image sensor," in *Proc. SPIE*, vol. 8255, 2012, p. 42. doi: 10.1117/12.907186.

[12] L. Kadura *et al.*, "Extending the functionality of FDSOI N- and P-FETs to light sensing," in *Proc. IEEE Int. Electron Devices Meeting (IEDM)*, 2016, pp. 1–4. doi: 10.1109/IEDM.2016.7838530.

[13] T. Nirschl *et al.*, "The 1T photo pixel cell using the tunneling field effect transistor (TFET)," in *Proc. IEEE Int. Electron Devices Meeting*, 2005, pp. 66–67.

[14] Q. Liu *et al.*, "Ultra-thin-body and BOX (UTBB) fully depleted (FD) device integration for 22nm node and beyond," in *Proc. IEEE VLSI Technol.*, 2010, pp. 61–62.

[15] J.-P. Noel, O. Thomas, C. Fenouillet-Beranger, M.-A. Jaud, P. Scheiblin, and A. Amara, "A simple and efficient concept for setting up multi-VT devices in thin BOx fully-depleted SOI technology," in *Proc. IEEE Eur. Solid-State Device Res. Conf.*, 2009, pp. 137–140.

[16] V. T. Itocazu, V. Sonnenberg, E. Simoen, C. Claeys and J. A. Martino, "Substrate effect on UTBB SOI nMOSFET," in *Proc. 28th Symp. Microelectron. Technol. Devices (SBMicro)*, Curitiba, Brazil, 2013, pp. 1–4. doi: 10.1109/SBMicro.2013.6676153.

[17] L. Grenouillet and M. Vinet, "UTBB CMOS IMAGER," U.S. Patent 20 130 113 066, May 9, 2013.

[18] *Sentaurus Device Manual*, Synopsys Inc. Mountain View, CA, USA, 2013.